

Theoretical investigation of hole transport in strained III-V semiconductors: Application to GaAs

J. M. Hinckley and J. Singh

Center for High Frequency Microelectronics, Department of Electrical Engineering and Computer Science, The University of Michigan, Ann Arbor, Michigan 48109-2122

(Received 21 April 1988; accepted for publication 23 June 1988)

A Monte Carlo method has been developed and applied to study the anisotropic transport of holes in unstrained and strained bulk III-V compound semiconductors. In this letter, we present the results for the prototypical GaAs, $T = 300$ K material system. We find that the hole mobility can be significantly increased by the presence of biaxial compressive strain in the system. This arises from strain-induced modifications in the densities of states and the overlap functions and from a separation of the heavy and light hole bands at $\mathbf{k} = 0$ which decreases the heavy to light hole interband scattering. For a 1.5% biaxial compressive strain, the hole mobilities are increased by up to a factor of 2 over the unstrained values. This improvement is sustained up to the highest field in our simulations which was 20 kV/cm.

The operation of many electronic and optoelectronic devices critically depends upon hole transport. Recent experimental evidence indicates that the incorporation of biaxial compressive strain in the heterostructure channel of p -type pseudomorphic modulation-doped field-effect transistors (MODFET's) leads to greatly enhanced carrier mobility.^{1,2} However, we find that relatively little work has been carried out in the area of accurate theoretical calculations of hole transport. From a theoretical point of view, hole transport is much more complex than electron transport because of the intrinsically anisotropic nature of the valence bands and eigenstates. The overlap function between the periodic part of the Bloch states describing the initial and final hole states involved in scattering becomes difficult to incorporate in a transport calculation. In the past, the $\mathbf{k}\cdot\mathbf{p}$ theory has been used to study hole transport, where the overlap functions used were simplified and analytical.³⁻⁷ However, to study the effect of strain on hole transport, a technique is required which can incorporate a more accurate description of the valence states and band structure. It should be able to (i) fully account for the symmetry and nonparabolicity features of the hole band structure and eigenstates, (ii) describe hole transport in the presence of arbitrary strain-induced modifications to the band structure and eigenstates, and (iii) describe transport in quasi-two-dimensional systems. In this letter, we present the results of using a Monte Carlo technique that we have developed, which meets the first two criteria and sheds some light on the third.

Customarily, charge carrier transport in a Monte Carlo calculation involves the evaluation of three major things⁸: (i) the overlap functions, (ii) the scattering rates and their angular dependence, and (iii) the transport properties such as drift velocity, carrier temperature, and distribution functions. The scattering rate by mechanism m [e.g., polar longitudinal optical (LO) phonon emission] of a hole initially in band n , with wave vector \mathbf{k} to a state in band n' , is given by

$$W_{m,n,n'}(\mathbf{k}) = \frac{V_c}{(2\pi)^3} \frac{2\pi}{\hbar} \int d^3k' |M_m(\mathbf{k},\mathbf{k}')|^2 G_{n,n'}(\mathbf{k},\mathbf{k}') \times \delta(E_n + \Delta E_m - E_{n'})$$

$$= \frac{V_c}{(2\pi)^3} \frac{2\pi}{\hbar} \int dk' d\Omega' T(\mathbf{k},\mathbf{k}'), \quad (1)$$

where $G_{n,n'}(\mathbf{k},\mathbf{k}')$ is the overlap function and $M_m(\mathbf{k},\mathbf{k}')$ is the matrix element of the scattering Hamiltonian \mathcal{H}_m between the initial and final state. The integrand $T(\mathbf{k},\mathbf{k}')$, Eq. (1), gives the angular distribution of the scattering process. The anisotropy of the hole bands precludes both expressing this as a function of $k_s = k' - k$ and expressing the scattering rate W as a function of wave vector magnitude only, as are done in the case of electron transport. We have retained the full wave vector dependence of both these types of quantities in our work.

To describe the valence band structure of GaAs at $T = 300$ K, we use the 6×6 Kohn-Luttinger Hamiltonian.⁹ Not only does this Hamiltonian provide a fairly accurate description of hole states up to 1 eV, near the top of the valence band, it also may be straightforwardly modified to describe the hole dispersion in MODFET's and other quantum well structures.¹⁰ A biaxial compressive strain in the (001) plane (which contains wave vectors lying in the directions [100] and [010]) is described by the strain tensor $\epsilon_{xx} = \epsilon_{yy} = \epsilon$, $\epsilon_{zz} = (-2c_{12}/c_{11})\epsilon$, $\epsilon_{xy} = \epsilon_{yz} = \epsilon_{zx} = 0$, $\epsilon > 0$. Such a strain causes a shift and a splitting in the diagonal terms of the Kohn-Luttinger Hamiltonian. This is represented by the additive diagonal terms in the Hamiltonian.¹¹ The heavy hole and light hole states are split by roughly 6.48 ϵ (eV)^{11,13} for GaAs at $T = 300$ K.

Figure 1 shows the band structure for GaAs in the absence and presence of biaxial compressive strain ($\epsilon_{xx} = \epsilon_{yy} = 0.015$). Note that near the band edge, the hole band becomes considerably lighter in the (001) plane (i.e., the [100] direction in the figure). This feature has been the motivation for the experimental work involving the use of biaxial compressive strain to enhance hole transport.

In Fig. 2 we show some typical overlap functions, $G_{n,n'}(\mathbf{k},\mathbf{k}')$, for the unstrained and strained cases. These

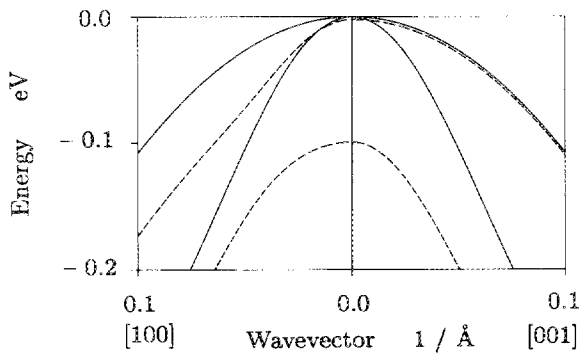


FIG. 1. Heavy and light hole dispersion relations from 6×6 Kohn-Luttinger Hamiltonian for $T = 300$ K GaAs. Unstrained (solid lines) and biaxially compressively strained with $\epsilon_{xx} = \epsilon_{yy} = 0.015$ (dashed lines).

have been calculated by taking the scalar product of the initial and final eigenvectors of the 6×6 Kohn-Luttinger Hamiltonian. This is an approximation which relies on the assumption that $(1/\Omega) \int_{\Omega} \exp[i(\mathbf{k}' - \mathbf{k}) \cdot \mathbf{r}] d^3r \approx 1$, where Ω is the volume of the unit cell of the Bravais lattice. At the moderate fields employed in the present work, \mathbf{k}' and \mathbf{k} are generally small, supporting the validity of this assumption. The anisotropic features of the lattice are retained in the solution and the strain-induced reduction of symmetry is evident in the figure.

The modulus squared matrix elements $|M_m(\mathbf{k}, \mathbf{k}')|^2$, for the various scattering mechanisms used in this work, are well known,¹⁴ and were combined with the overlap functions and density of final states to determine the scattering rates and their angular distributions. Twenty scattering mechanisms have been considered in this work: polar optical phonon emission and absorption, acoustic phonon scattering, and nonpolar optical phonon emission and absorption, each of which may drive heavy to heavy, heavy to light, light to heavy, or light to light hole band transitions. Figure 3

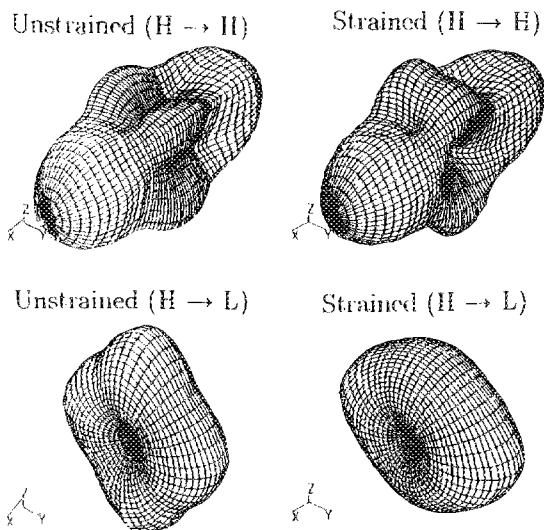


FIG. 2. Polar plots of representative heavy hole overlap functions, $G_{m,n}(\mathbf{k}, \mathbf{k}')$, as a function of the direction of the final wave vector. In all cases shown, the initial wave vector is in the $[100]$ (X) direction and both the initial and final energies are -0.15 eV relative to the top of the heavy hole band.

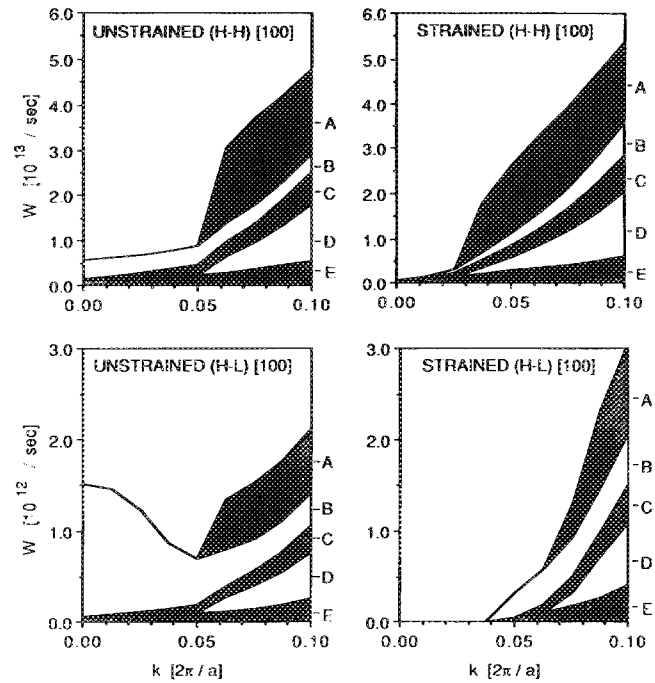


FIG. 3. Heavy hole scattering rates for intraband ($H-H$) and interband ($H-L$) transitions in both the unstrained and biaxially compressively strained ($\epsilon_{xx} = \epsilon_{yy} = 0.015$) cases for $T = 300$ K GaAs. The initial wave vector is in the $[100]$ direction. A, B: polar optical phonon emission, absorption; C: acoustic phonon scattering; D, E: nonpolar optical phonon emission, absorption.

shows the heavy hole scattering rates in both the unstrained and strained GaAs material at $T = 300$ K. The rates are shown for an initial wave vector aligned in the $[100]$ direction. The strain-induced valence band splitting at $\mathbf{k} = 0$ causes the suppression of the heavy hole to light hole interband transitions. This suppression, along with the modified densities of states and overlap functions, quantitatively changes the scattering rates and angular distributions for the holes in the strained system.

Finally, in Fig. 4 we show the velocity-field relations for hole transport in the unstrained and strained cases. In agreement with other studies,⁷ the hole transport in the unstrained system is essentially independent of electric field orientation. However, we find a significant increase of hole mobility in the strained system as the orientation of the field moves farther from the $[001]$ direction, and closer to the $[100]$ direction. The improvement exists over the entire range of our simulations (up to 20 kV/cm), as can be seen from the figure. For $E = 20$ kV/cm in the $[100]$ direction, the unstrained system had a population weighted average hole energy gain of 0.038 eV, with 92.5% of the holes in the heavy hole band, while the corresponding values for the strained system were 0.077 eV and 98.7% heavy holes.

At the moderate field of $E = 10$ kV/cm in the $[100]$ direction, the relative scattering frequencies for the unstrained heavy hole are 47% polar optical phonon ($H \rightarrow H$), 47% deformation potential scattering ($H \rightarrow H$), and 6% interband scattering ($H \rightarrow L$). The interband transitions ($H \rightarrow L$) are dominated by 48% polar optical phonon absorption. The unstrained light hole scattering has 85% inter-

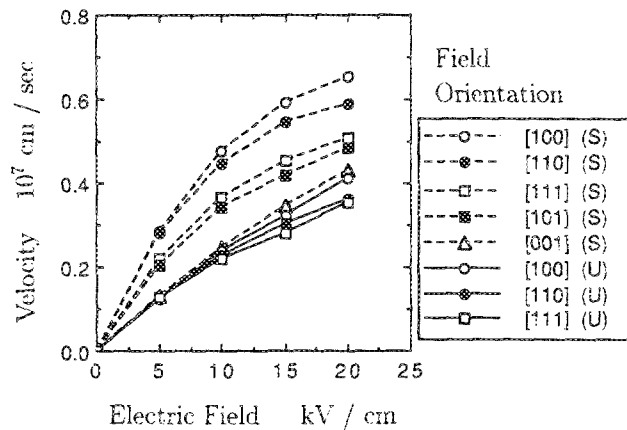


FIG. 4. Hole drift velocity-field characteristics for both the unstrained (U) and biaxially compressively strained (S) ($\epsilon_{xx} = \epsilon_{yy} = 0.015$) cases for $T = 300$ K GaAs. The three lowest velocity traces are for unstrained material (solid lines), while the upper five traces are for 1.5% strained material (dashed lines).

band transitions ($L \rightarrow H$), 45% of which are by polar optical phonon emission alone. For the strained system the heavy hole relative scattering frequencies are 61% polar optical phonon ($H \rightarrow H$), 38% deformation potential scattering ($H \rightarrow H$), and 1% interband scattering ($H \rightarrow L$). 32% of the interband transitions ($H \rightarrow L$) are via polar optical phonon absorption. 76% of the strained light hole scatterings are interband transitions ($L \rightarrow H$), 32% of which are polar optical phonon emission. While the present work considers only a bulk system, it does have qualitative agreement with strained quasi-two-dimensional transport as implied from strained-layer MODFET behavior.^{1,2} Mobility is enhanced by the presence of compressive biaxial strain in the plane containing the direction of drift motion.

In summary, we have developed and implemented a general technique to study hole transport in anisotropic, strained bulk systems. Substantial increases in hole mobility may be found from our calculations. The approach presented in this letter may be straightforwardly modified to investigate both strains in other crystallographic orientations and the dynamics of quasi-two-dimensional structures. Because hole transport is often a limiting feature for many optoelectronic and electronic devices, the present technique offers a useful first step guideline in device design. Finally, many devices may be successfully modeled as bulk materials. However, the extension of this technique, by the inclusion of correct quasi-two-dimensional physics, will be necessary to obtain quantitative descriptions of the behavior of devices such as p -MODFET's. We have begun work on this.

This work was supported by the U.S. Army Research Office (grant DAAL03-87-K-0007).

- ¹T. E. Zipperian, L. R. Dawson, T. J. Drummond, J. E. Schirber, and I. J. Fritz, *Appl. Phys. Lett.* **52**, 975 (1988).
- ²C. P. Lee, H. T. Wang, G. J. Sullivan, N. H. Sheng, and D. L. Miller, *IEEE Electron. Device Lett.* **EDL-8**, 85 (1987).
- ³J. D. Wiley, *Phys. Rev. B* **4**, 2485 (1971).
- ⁴M. Costato and L. Reggiani, *Phys. Status Solidi B* **58**, 461 (1973).
- ⁵M. Costato and L. Reggiani, *Phys. Status Solidi B* **59**, 47 (1973).
- ⁶D. Kranzer, *Phys. Status Solidi A* **26**, 11 (1974).
- ⁷K. Brennan and K. Hess, *Phys. Rev. B* **29**, 5581 (1984).
- ⁸W. Fawcett, A. D. Boardman, and S. Swain, *J. Phys. Chem. Solids* **31**, 1963 (1970).
- ⁹J. M. Luttinger and W. Kohn, *Phys. Rev.* **97**, 869 (1955).
- ¹⁰G. Bastard and J. A. Brum, *IEEE J. Quantum Electron.* **QE-22**, 1625 (1986).
- ¹¹H. Kato, N. Iguchi, S. Chika, M. Nakayama, and N. Sano, *J. Appl. Phys.* **59**, 588 (1986).
- ¹²S. Adachi, *J. Appl. Phys.* **58**, R1 (1985).
- ¹³J. D. Wiley, *Solid State Commun.* **8**, 1865 (1970).
- ¹⁴B. R. Nag, *Electron Transport in Compound Semiconductors* (Springer, New York, 1980), p. 114.